Novel Nonreciprocal Devices with Integrated Electromagnet for Silicon Photonics

Paolo Pintus[(1,2)]*, Duanni Huang[(1)], Chong Zhang[(1)], Yuya Shoji[(3)],
Tetsuya Mizumoto[(3)], John E. Bowers[(1)]

[(1)] Dept. of Electrical and Computer Engineering, University of California, Santa Barbara, CA, USA,
[(2)] Istituto TeCIP, Scuola Superiore Sant'Anna, Pisa, Italy,
[(3)] Dept. of Electrical and Electronic Engineering / FIRST, Tokyo Institute of Technology, Tokyo, Japan
*e-mail: paolo.pintus@sssup.it

Abstract *We present a novel approach to construct integrated isolators and circulators based on magneto-optical materials. An integrated electromagnet is designed and fabricated, eliminating the need for a permanent magnet. The fabricated devices exhibit high performance and can be easily integrated/packaged.*

Introduction

Nonreciprocal components, such as optical isolators and circulators, are fundamental building blocks in optics to avoid undesirable back-reflections and to separate counter-propagating optical signals. In integrated optics, their fabrication is still very challenging and several approaches have been proposed.

Nonreciprocal devices are characterized by a symmetry breaking for the light that propagates from different directions, which results in a nonreciprocal scattering matrix [1]. Three different approaches can perform this work: i) nonlinear materials, ii) time modulation of the refractive index, iii) magneto-optic (MO) materials. However, only a few nonlinear optical phenomena such as Brillouin-scattering can be effectively used to break the symmetry, and silicon lacks a Pockels effect for efficient modulation [2,3]. On the other hand, MO material can be effectively bonded on silicon-on-insulator (SOI) wafer and the experimental results look very promising [4,5].

The MO material becomes nonreciprocal when it is in a quasi-static magnetic field. When light is transmitted through a magnetized medium, it exhibits a different phase velocity. Properly designed interferometric devices generate constructive interference for forward light and destructive interference for backward light achieving the isolating function [4,5]. However, the large absorption loss (e.g., 60dB/cm) in MO garnet and the use of a permanent magnet for applying an external magnetic field are two important aspects that limit the performance and the integration of those devices.

While the propagation loss can be greatly reduced in a device with small footprint, the external biasing magnet is still a significant limiting factor due to possible magnetic field interference with electronics and its large footprint (size>1mm) [4].

In this work, we investigate integrated optical isolators and circulators using a planar spiral electromagnet that provides local control of the magnetic field, and can be easily integrated and packaged. We then experimentally verify our model and explore the implications of these novel devices.

Proposed device

The proposed devices are shown in Fig. 1. A silicon ring resonator is fabricated on a SOI wafer, having refractive index n_{Si}=3.48 and n_{SiO2}=1.46 at λ=1550nm, respectively. The ring is bonded with a Ce:YIG garnet ($n_{Ce:YIG}$=2.22) grown on a (Ca,Mg,Zr)-substituted gadolinium gallium garnet (SGGG), ($n_{Ce:YIG}$=1.97), whereas the remaining space is filled by air.
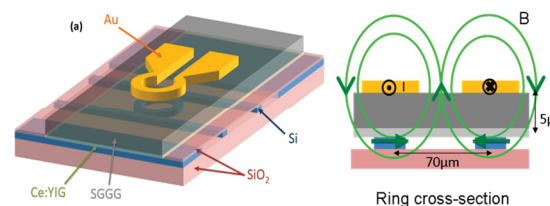
Fig. 1: (a) Perspective view and (b) cross-sectional view of a proposed optical circulator with integrated electromagnet.

The silicon waveguide cross-section (230nm × 600nm) has been designed to maximize the nonreciprocal resonance split between the clockwise (CW) and the counter-clockwise (CCW) transverse magnetic (TM) mode [6,7]. Due to the high SOI index contrast, a high field confinement factor can be achieved even with rather small ring radius (i.e., R=35μm). This small footprint of the device has allowed us to reduce the total excess loss down to 2.3dB [9].

Using a mechanical lapping technique, the SGGG substrate on the bonded die can be thinned down to 5μm and a Ti/Au metal layer is patterned onto the back-side of the SGGG

substrate using i-line lithography and metal liftoff. The electromagnet is fabricated using a 1.5µm thick and 3.0µm wide gold microstrip. By injecting a DC current into the metal coil, a magnetic field is locally applied. In order to increase the magnetic field intensity without increasing the electrical current, a planar spiral solution is investigated. For this purpose, 2 layers of metal are needed and the minimum microstrip separation in the spiral is set to 1.0µm.

Mathematical model

When a static radial magnetic field is applied, the CW and the CCW modes in the ring have a different effective index and a split between their resonance wavelengths occurs, and is given as

$$\Delta \lambda_M^0 = \frac{\Delta n_{eff}}{n_g} \lambda \qquad (1)$$

where Δn_{eff} is the effective index variation and n_g is the average group index with respect to the two directions computed at room temperature. For the device under investigation, we expected a resonance wavelength split $\Delta \lambda_M^0$ =0.52nm [4,9]. This value is proportional to the Faraday rotation constant θ_F. At room temperature, the Faraday rotation can be approximated with an hyperbolic tangent

$$\theta_F = \theta_F^0 \cdot \tanh\left(\frac{H_r}{1440[Oe]}\right) \qquad (2)$$

where θ_F^0 =-4500°/cm is the saturation value, which is reached for H_r>50 Oe [4].

The DC current used to generate the magnetic field might also causes a local heating of the silicon ring, due to the Joule effect. By performing the electromagnetic modal analysis of the ring with respect to the temperature, the thermal resonance wavelength shift $\Delta \lambda_T$ is valued as

$$\Delta \lambda_T = \frac{\lambda}{n_g}\left(\sum_i \frac{\partial n_{eff}}{\partial n_i} \frac{\partial n_i}{\partial T}\right)\Delta T \qquad (3)$$

where the derivative $\partial n_i/\partial T$ depends on the materials with refractive index n_i, while $\partial n_{eff}/\partial n_i$ can be computed from the mode solver [7]. For the device under investigation, we calculate a resonance wavelength shift of 0.0716 nm/°C for the TM mode.

Due to the temperature variation, θ_F changes so the MO resonance wavelength split is

$$\Delta \lambda_M (H_r,T) = \frac{\Delta \lambda_M^0}{\theta_F^0}\left[\theta_F(H_r) + \frac{d\theta_F}{dT} \cdot \Delta T\right] \qquad (4)$$

where H_r is the radial magnetic field. As the device heats up, the Faraday rotation will

change by $d\theta_F/dT$=+44 deg/°C [8]. Combining these two effects, we find that the total resonance wavelength shift is

$$\Delta \lambda = \Delta \lambda_T(T) \pm \frac{1}{2}\Delta \lambda_M(H_r,T) \qquad (5)$$

where ± refer to the CW and CCW modes, respectively.

Numerical Results

The radial magnetic field H_r and the temperature distribution T have been computed using COMSOL Multiphysics software. In Fig. 2, the numerical results are reported for the 3 loop spiral integrated planar electromagnet. The intensity of the radial magnetic field at the Si/Ce:YIG interface is shown in Fig. 2a assuming 180 mA DC current, while in Fig.2b the temperature distribution is shown for the same device under the same condition. From both images, it is clear that the magnetic field and temperature variation are local and do not affect devices that are relatively far from it.
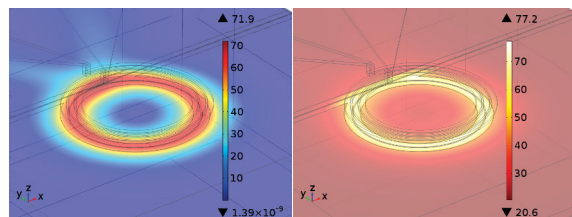

Fig. 2: Multiphysics simulation results: a) radial magnetic field generated by the electric current I=180 mA, b) temperature distribution in the device

The performance of single loop, 3-loops and 5-loops are compared in Fig. 3. The magnetic field in the Ce:YIG (5µm far from metal layer) is computed as a function of the injected current. For the same value, the temperature in the silicon is reported in Fig. 3b. Those simulations results can be effectively used to compute the thermal shift (reciprocal) and the magneto-optical split (nonreciprocal) described by Eq. (3) and Eq. (4), respectively.

Experimental Verification

We experimentally validate the model by testing a nonreciprocal all-pass ring resonator with a single electromagnet coil. We record the transmittance of the device as we sweep the tunable laser wavelength, and repeat the
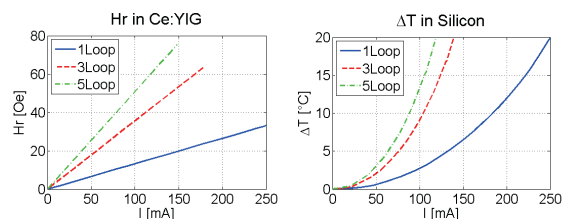

Fig. 3: Electromagnet comparison a) radial magnetic field at the silicon-Ce:YIG interface b) average temperature variation in the silicon ring

measurements for backwards transmission. In Fig. 4, we see a clear resonance split of roughly 0.32nm between the forward and backwards propagating light for 140mA of applied current (roughly 20 Oe of applied field). There is also a thermally induced redshift of 0.4 nm between the resonance when no current and field is applied, and the average of the CW and CCW resonances under the magnetic field.
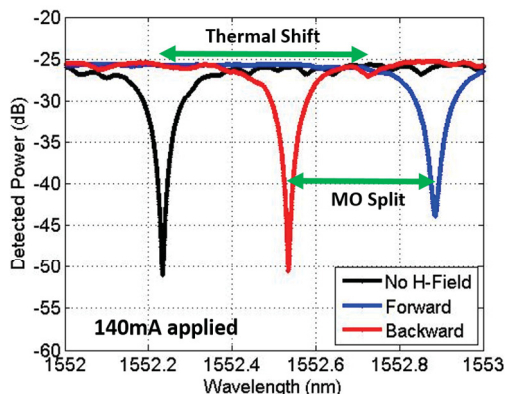
Fig. 4: Experimental results showing both the nonreciprocal MO wavelength split as well as the thermally induced redshift.

This set of measurements is repeated for current values between 0 and 220mA, and the results are compared with the simulations. We report very good agreement between experimental and numerical results for the single loop electromagnet, as shown below in Fig. 5. The slight deviation from the numerical results can be attributed to the SGGG thickness not being exactly 5 micrometers.

Nonetheless, it is clear from Fig. 5 that increasing the number of spiral loops in the electromagnet will allow us to obtain MO wavelength split, up to the previously predicted 0.52nm. Furthermore, it will greatly decrease the amount of current required for a wavelength split, which eases the requirements for accompanying CMOS drivers. Finally, the combination of the electromagnet (low resistance) with a separate thermal heater (higher resistance) can result in a wider tuning range for the devices. This is important considering the microring isolator and circulators are intrinsically narrowband.
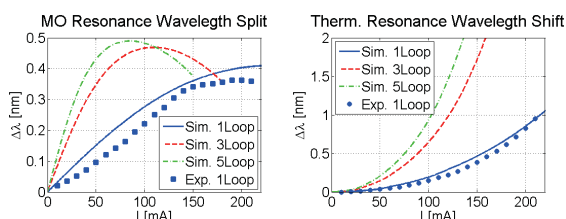
Fig. 5: Electromagnet comparison a) MO resonance wavelength split b) thermal resonance wavelength shift

Conclusions

In this work, we show that the proposed electromagnet can be used to provide a local control of the magnetic field. Thus, we eliminate the need for a bulky permanent magnet, which increases footprint and complicates packaging. Moreover, using a multi-loop spiral solution, we have been able to reduce the current needed for a large MO split, which is necessary for high optical isolation. Finally, the current induced magnetic field can be switched and modulated, possibly leading to a new class of magneto-optic devices for silicon photonics.

Acknowledgements

References

[1] D. Jalas et al., "What is - and what is not - an optical isolator", Nat. Photonics, Vol. **7**, no. 8, p. 579, (2013).

[2] Y. Shi et al., "Limitations of nonlinear optical isolators due to dynamic reciprocity", Nat. Photonics, Vol. **9**, no. 6, p. 388, (2015).

[3] C. Dong et al., "Brillouin-scattering-induced transparency and non-reciprocal light storage", Nat. Communications, Vol. **6**, p. 6193, (2015).

[4] M. Tien, T. Mizumoto, P. Pintus, H. Kromer, and J.E. Bowers, "Silicon ring isolators with bonded nonreciprocal magneto-optic garnets", Opt. Express, Vol. **19**, no. 12, p. 11740, (2011).

[5] Y. Shoji, M. Ito, Y. Shirato, and T. Mizumoto, "MZI optical isolator with Si-wire waveguides by surface-activated direct bonding", Opt. Express, Vol. **20**, no. 16, p. 18440, (2012).

[6] P. Pintus, M. Tien, and J.E. Bowers, "Design of Magneto-Optical Ring Isolator on SOI Based on the Finite-Element Method", IEEE Photon. Technol. Lett., Vol. **23**, no. 22, p. 1670, (2011).

[7] P. Pintus, "Accurate vectorial finite element mode solver for magneto-optic and anisotropic waveguides", Opt. Express, Vol. **22**, no. 13, p. 15737, (2014).

[8] K. Furuya, T. Nemoto, K. Kato, Y. Shoji, T. Mizumoto, "Athermal operation of a waveguide optical isolator based on canceling phase deviations in a Mach-Zehnder interferometer", J. Lightwave Technology,Vol. **34**, No. 8, p. 1699, (2016).

[9] D. Huang, P. Pintus, C. Zhang, Y. Shoji, T. Mizumoto, and J. Bowers, "Silicon microring isolator with large optical isolation and low loss," in Optical Fiber Communication Conference, Th1K.2, (2016).